Pharmaceutical Biology

ISSN: (Print) (Online) Journal homepage: www.informahealthcare.com/journals/iphb20

Babaodan overcomes cisplatin resistance in cholangiocarcinoma via inhibiting YAP1

Jiong Li, Xiangjun Ma, Faying Xu, Yuanliang Yan & Weiqing Chen

To cite this article: Jiong Li, Xiangjun Ma, Faying Xu, Yuanliang Yan & Weiqing Chen (2024) Babaodan overcomes cisplatin resistance in cholangiocarcinoma via inhibiting YAP1, Pharmaceutical Biology, 62:1, 314-325, DOI: 10.1080/13880209.2024.2331060

To link to this article: https://doi.org/10.1080/13880209.2024.2331060

PHARMACEUTICAL BIOLOGY
2024, VOL. 62, NO. 1, 314–325
https://doi.org/10.1080/13880209.2024.2331060

Taylor & Francis
Taylor & Francis Group

RESEARCH ARTICLE

Babaodan overcomes cisplatin resistance in cholangiocarcinoma via inhibiting YAP1

Jiong Li[a], Xiangjun Ma[a], Faying Xu[b], Yuanliang Yan[c*] and Weiqing Chen[d*]

[a]Department of Traditional Chinese Medicine, The First People's Hospital of Lin'an District, Hangzhou, China; [b]College of Clinical Medicine, Hangzhou Medical College, Hangzhou, China; [c]Department of Pharmacy, Xiangya Hospital, Central South University, Changsha, Hunan, China; [d]Department of General Surgery, The First People's Hospital of Lin'an District, Hangzhou, China

ABSTRACT

Context: Cholangiocarcinoma with highly heterogeneous, aggressive, and multidrug resistance has a poor prognosis. Although babaodan (BBD) combined with cisplatin improved non-small cell lung cancer efficacy, its impact on overcoming resistance in cholangiocarcinoma remains unexplored.

Objective: This study explored the role and mechanism of BBD on cisplatin resistance in cholangiocarcinoma cells (CCAs).

Materials and methods: Cisplatin-resistant CCAs were exposed to varying concentrations of cisplatin (25–400 μg/mL) or BBD (0.25–1.00 mg/mL) for 48 h. IC_{50} values, inhibition ratios, apoptosis levels, DNA damage, glutathione (GSH) levels, oxidized forms of GSH, total GSH content, and glutaminase relative activity were evaluated using the cell counting kit 8, flow cytometry, comet assay, and relevant assay kits.

Results: BBD-reduced the cisplatin IC_{50} in CCAs from 118.8 to 61.83 μg/mL, leading to increased inhibition rate, apoptosis, and DNA damage, and decreased expression of B-cell lymphoma-2, p-Yes-associated protein 1/Yes-associated protein 1, solute carrier family 1 member 5, activating transcription factor 4, and ERCC excision repair 1 in a dose-dependent manner with maximum reductions of 78.97%, 51.98%, 54.03%, 56.59%, and 63.22%, respectively; bcl2-associated X and gamma histone levels were increased by 0.43–115.77% and 22.15–53.39%. The impact of YAP1 knockdown on cisplatin-resistant CCAs resembled BBD. GSH, oxidized GSH species, total GSH content, and glutaminase activity in cisplatin-resistant CCAs with BBD treatment also decreased, while YAP1 overexpression countered BBD's effects.

Discussion and conclusion: This study provides a scientific basis for BBD clinical application and provides a new direction for BBD biological mechanism research.

ARTICLE HISTORY
Received 17 July 2023
Revised 5 March 2024
Accepted 6 March 2024

KEYWORDS
Apoptosis; DNA damage; glutathione; yes-associated protein 1

Introduction

Cholangiocarcinoma (CCA) is a rare and aggressive biliary cancer known for its significant heterogeneity (Guedj 2022). This malignancy is categorized into three primary types based on its location within the biliary tree: intrahepatic CCA, perihilar CCA, and distal CCA (Rodrigues et al. 2021). Global incidence rates of CCA are increasing, representing 15% of primary liver cancers and 3% of gastrointestinal malignancies. As a result, CCA is the second most prevalent primary liver cancer, trailing only hepatocellular carcinoma (Banales et al. 2020). Multiple factors, such as liver cirrhosis, hepatolithiasis, obesity, diabetes, and metabolic syndrome, have been implicated as potential risk factors for CCA. The complex and heterogeneous nature of CCA has hindered the definitive identification of these risk factors (Khan et al. 2019). The preferred treatment strategy for CCA is surgical resection (Rizvi et al. 2018). However, most CCA patients have missed the optimal stage of surgery when diagnosed due to its invasive nature (Dwyer et al. 2021). In these cases, systemic chemotherapy is usually the only treatment option. However, due to drug resistance, the long-term prognosis for CCA remains poor (Zheng et al. 2022). Therefore, therapeutic strategies must be developed to combat resistance to CCA (Prasopporn et al. 2022).

Cisplatin has multiple mechanisms of anticancer activity. The most common pathways include the generation of DNA lesions through interaction with purine bases in DNA, followed by the activation of several pathways leading to apoptosis (Ghosh 2019). The cisplatin-induced apoptotic response was found to be reduced in the presence of the reactive oxygen species glutathione (GSH) scavenger (Kleih et al. 2019). GSH synthesis plays a significant role in cisplatin resistance. Resistant cells generally exhibit elevated GSH (Kobayashi et al. 2022). In cisplatin-resistant hepatocarcinoma cells, the GSH content increased twice compared to the ordinary hepatocarcinoma cell line (Jia et al. 2012). Cisplatin resistance in biliary tract cancer was reversed by decreasing the GSH and the GSH/oxidized GSH (GSSG) ratio (Li et al. 2016). Additionally, the knockdown of Yes-associated protein 1 (YAP1) attenuated chemoresistance in bladder cancer cells (Ciamporcero et al. 2018). YAP1 is a key effector molecule downstream of the Hippo signaling pathway, capable of

CONTACT Weiqing Chen cwq19810501123@sina.com Department of General Surgery, The First People's Hospital of Lin'an District, No. 548, Yijin Street, Jincheng Street, Lin'an District, Hangzhou, 311300 Zhejiang, China; Yuanliang Yan yanyuanliang@csu.edu.cn National Clinical Research Center for Geriatric Disorders, Xiangya Hospital, Central South University, Changsha, 410008 Hunan, China
*These authors contributed equally to this work.

Supplemental data for this article can be accessed online at https://doi.org/10.1080/13880209.2024.2331060.

regulating the expression of various genes related to GSH synthesis (Mohajan et al. 2021). A study reported (Gao et al. 2021) that YAP1 provided the raw materials necessary for GSH synthesis by increasing the expression of the solute carrier family 7 member 11 (SLC7A11). Therefore, YAP1 can promote drug resistance in cholangiocarcinoma cells by regulating GSH, leading to the deterioration of the disease.

Traditional Chinese medicine (TCM), such as Yinchenhao decoction and the Chinese skullcap, has shown its potential to prevent and treat CCA (Chen Z et al. 2021). Babaodan (BBD), the TCM formula produced in China's Fujian province, originated in the Ming dynasty (Wang et al. 2019). The BBD formula includes *Radix* of *Panax notoginseng (Burkill)* F.H.Chen [Araliaceae] and other precious TCM and has been approved by the China Food and Drug Administration. The main chemical components of BBD include saponins, bile acids, and amino acids (Zheng Y et al. 2022). Evidence suggests that BBD has anti-inflammatory and antitumor activity (Zhao et al. 2021). The active ingredient of *Panax notoginseng* and ginsenoside compound K inhibited the growth of hepatocellular carcinoma by regulating YAP1 phosphorylation (Zhang J et al. 2022). It can enhance the antitumor activity of cisplatin in non-small cell lung cancer (Wang et al. 2019). Liu J et al. (2020) reported an inhibitory effect of BBD on gastric cancer cells. Furthermore, BBD can antagonize cisplatin resistance in gastric cancer cells by regulating apoptosis and autophagy (Zhao et al. 2021).

However, the biological mechanism of BBD on CCA is still unclear. Its exploration can provide a research basis for tumor treatment, which is conducive to developing clinical treatment strategies for CCA and the clinical application of BBD. This study used cisplatin-resistant cell lines intervened with BBD (0.25, 0.5, and 1 mg/mL) or with YAP1 knockdown to explore the effects and mechanism of BBD to improve the sensitivity of CCA cells to cisplatin.

Materials and methods

Cisplatin-resistant cell lines

Human cholangiocarcinoma cells (RBE cells, RRID: CVCL_4896; Cat# CL-0191, Procell, Wuhan, China) were cultured in a complete medium containing phenol-free RPMI-1640 (Cat# 11835030, Gibco, USA) with 10% FBS (Cat# 11012-8611, Every Green, China) and 1% penicillin-streptomycin solution (Cat# 15140122, Gibco, USA) and placed in a standard cell culture environment with 5% CO_2 at 37 °C. Cells were exposed to 1 μM cisplatin (Cl2H6N2Pt, Cat# 232120, CAS: 15663-27-1, > 98.0% purity, Sigma–Aldrich, USA) for 72 h in the culture flask to establish cisplatin-resistant cells as previously reported (Liu CW et al. 2017). Cells were then cultured in a complete medium for recovery. The above process was repeated five times. Cisplatin was dissolved in NaCl and diluted to desired concentrations in a complete medium.

Drug treatment and grouping

CCAs resistant to cisplatin were treated with different doses of cisplatin (25, 50, 100, 200, and 400 μg/mL) to calculate the IC_{50}. This dose of IC_{50} was then used for subsequent experiments (Zhao et al. 2021). Normal cultured cisplatin-resistant cells and cells that were incubated with a complete medium containing cisplatin or cisplatin and BBD (0.25, 0.5, and 1 mg/mL, Xiamen Traditional Chinese Medicine, China) for 48 h were used to observe the effect of BBD on cisplatin-resistant CCAs. The cells were categorized into distinct groups: the control group, which solely received cisplatin (CDDP) at a dose equivalent to the IC_{50} (118.8 mg/mL), and experimental groups including cisplatin combined with BBD at varying concentrations: cisplatin + 0.25 mg/mL BBD (CDDP + 0.25 BBD), cisplatin + 0.5 mg/mL BBD (CDDP + 0.5 BBD), and cisplatin + 1 mg/mL BBD (CDDP + 1 BBD). These groupings were implemented to assess the counteractive effects of BBD on cisplatin-resistant CCAs. The BBD was diluted in PBS to the desired concentrations in the complete medium.

Cisplatin-resistant CCAs were transfected with an empty plasmid vector, siNC, a plasmid with YAP1 cDNA, and siYAP1 using lipofectamine 3000 (Cat# L3000075, Thermos Fisher, USA). Plasmid, siRNA, and their negative control were designed and synthesized by GeneChem Co., Ltd, Shanghai, China. These cells were divided into four groups: 1) the CDDP group: cells were cultured in a complete medium supplemented with cisplatin. They were transfected with an empty plasmid vector and siNC (non-targeting control); 2) the CDDP + siYAP1 group: cells were subjected to YAP1 silencing and treated similarly to the CDDP group; 3) the CDDP + BBD group: cells were cultured in a complete medium supplemented with cisplatin and exposed to 1 mg/mL of BBD; and 4) the CDDP + BBD + YAP1 group: cells that had YAP1 overexpression were cultured similarly as the CDDP + BBD group.

Inhibition rate and IC_{50} value of cisplatin-resistant CCAs

The inhibition rate and IC_{50} were measured using the cell counting kit 8 (CCK8) (Cat# C0039, Beyotime, Shanghai, China). In 96-well cell culture plates (5×10^3 cells/well), cells were incubated for 24 h to attach to the well surface. The cell culture medium per well was replaced with a complete culture medium (phenol-free) containing 10 μL CCK8 incubation for 1 h. Finally, the optical density (OD) was measured at 450 nm using a microplate reader (CMaxPlus, Molecular Devices, USA). Inhibition rate= [(OD of the control group - OD of the experimental group)/(OD of the control group-black group)] × 100%. Additionally, the reversal fold (RF), calculated as RF = IC_{50} (cisplatin)/IC_{50} (cisplatin with 1 mg/mL BBD treatment), was used to compare the sensitivity of CCAs to cisplatin (Zhao et al. 2021).

Total RNA extraction

After cell transfection and cultivation for 48 h, total RNA was extracted using an EZ-10 DNAaway RNA Mini-Preps kit (Cat# B618583-0100, Sangon Biotech, China) containing spin column, tubes, DW/RPE solutions, RNase-free water, and lysis buffer. Briefly, 300 μL lysis buffer was used to lysate cells followed by collecting into a spin column. Then, 150 μL ethanol was added and transferred to a 2 mL RNase-free collection tube for centrifuging at 12 000 × g, for 2 min at room temperature. The filtrate was discarded and added 350 μL DW solution, followed by centrifuging at 12 000 × g for 1 min at room temperature. Subsequently, the filtrate was discarded again, and 500 μL RPE Solution was added and centrifuged at 12 000 × g for 1 min at room temperature. Subsequently, the column was recentrifuged and then kept until the ethanol evaporated completely. The sample was dissolved in 30 μL RNase-free water and purity was detected using a NanoDrop one-trace UV Vis spectrophotometer

(Thermo Scientific, USA). Subsequently, the sample was reverse transcribed to cDNA using a CWBIO's kit (Cat# CW2569, CWBIO, China; Reaction conditions: 42 °C for 15 min; 85 °C for 5 min).

Quantitative real-time PCR

Quantitative real-time PCR (qPCR) was performed using a qPCR kit (Cat# 11201ES08, Yeasen, China) on the LightCycler 96 real-time PCR system (Roche, Switzerland). Reaction conditions are 95 °C for 5 min, 40 cycles of 95 °C for 10 s, and 60 °C for 60 s. Following primer pairs were used for qPCR: YAP1 forward, 5′-TAGCCCTGCGTAGCCAGTTA-3′, Reverse, 5′-TCATGCTTAG TCCACTGTCTGT-3′; GAPDH forward, 5′-ACAACTTTGGTATC GTGGAAGG-3′, Reverse, 5′-GCCATCACGCCACAGTTTC-3′. The primers were synthesized by Sangon Biotech Co., Ltd, Shanghai, China. Results were normalized to housekeeping gene GAPDH. The relative expression of genes was calculated by $2-\triangle\triangle^{C}_{t}$ method.

Flow cytometry

After cell processing according to the grouping requirements, cells were harvested and washed with PBS, mixed in 100 µL of 1× binding buffer, and stained with Annexin V/propidium iodide (PI) double staining solution (Cat# 556547, BD Biosciences, USA) for 15 min at 37 °C. Cell apoptosis was detected by flow cytometry (NovoCyte, Agilent, Germany). Cell apoptosis was assessed by flow cytometry. The gating strategy for apoptotic cells was based on forward and side scatter results, control cells and single stained cells. Briefly, forward and side scatter characteristics (FSC-H and SSC-H) were used to exclude debris. Control tubes contained blank cells, Annexin V-FITC single-stained cells and PI single-stained cells, facilitated the adjustment of flow cytometric compensation. The flow cytometry results from the blank control were used to confirm the presence of negative cells. In contrast, the results from the Annexin V-FITC single-stained and PI single-stained were used to define the Y-axis and X-axis, respectively. Cells that stained positive for Annexin V-FITC only were identified as early apoptotic cells. In contrast, those that staining positively for both Annexin V-FITC and PI were categorized as late apoptotic cells. The quantification of apoptosis levels involved counting cells in the upper right quadrant (indicative of late apoptotic cells) and low right quadrant (representative of early apoptotic cells) in the flow cytometry dot plots.

GSH-related detection

Digested cells were used to measure GSH/GSSG and total GSH (TTGSH) according to the instructions of the GSH and GSSG kits (Cat# S0053, Beyotime, China). Briefly, fresh cells after grouping treatment were collected for cell precipitation. A protein or GSH removal reagent was added to cell precipitation followed by rapid freezing-thawing and centrifuging (with 10 000 × g at 4 °C for 10 min). The absorbance of the supernatant was detected in a 6-well plate at 412 nm using a microplate reader (CMaxPlus, Molecular Devices, USA). GSH = Total Glutathione-GSSG × 2. The glutaminase (GLS) activity assay was measured as previously reported (Chen P et al. 2021) according to the instructions of the GLS activity assay kit (Cat# BC1450, Solarbio, China). Extraction solution (200 µL) containing 10^5 cells was performed ultrasound followed by centrifuging (with 12 000 × g at 4 °C for 15 min). The supernatant is mixed with the working solution for measuring absorbance at 630 nm using a microplate reader. Reduced GSSG or GLS standard solution ranging from 1.25 mM to 0.125 µM was used to construct the standard curve.

Comet assay

The comet assay was performed to observe DNA damage from CCAs (Zong et al. 2019). Briefly, using the DNA Damage Assay Kit (Cat# PH9143, PHYGENE, China), cells were collected and mixed with low melting point agarose (v/v = 1:10) on a pre-coated 3-well Comet slide. Sequentially, pre-chilled lysis buffer and alkaline solution were used to treat the cells for 60 and 30 min at 4 °C in the dark. This preparatory step was conducted to facilitate subsequent electrophoresis, which was executed for 10 min. After staining with propidium iodide from comet assay kits, the slide was observed under a fluorescence microscope (Ts2-FL, Nikon, Japan). The tail moment and tail DNA were used to estimate DNA damage.

Western blot

Western blot was performed as previously described (Liu Z et al. 2018) after extracting total protein from the cells. The proteins in the samples were separated by electrophoresis and then transferred to a poly(vinylidene fluoride) membrane. The membrane was washed and incubated with primary antibodies overnight at 4 °C. Subsequently, the goat anti-rabbit IgG, HRP-linked antibody (1:3000; Cell Signaling Technology Cat# 7074, RRID: AB_2099233; USA) was used to incubate the membrane for 1 h at 25 °C. Protein bands were detected to measure the signal expression strength of B-cell lymphoma-2 (Bcl-2) (26 kDa, Rabbit polyclonal antibody) (1:2000; Affinity Biosciences Cat# AF6139, RRID: AB_2835021; USA), Bcl2-associated X (Bax) (21 kDa, Rabbit monoclonal antibody) (1:2000; Abcam Cat# ab182733, RRID: AB_2938987; UK), cleaved-caspase-3 (cle-caspase-3) (17 kDa, Rabbit monoclonal antibody) (1:500; Abcam Cat# ab32042, RRID: AB_725947), caspase-3 (34 kDa, Rabbit polyclonal antibody) (1:500; Abcam Cat# ab13847, RRID: AB_443014), p-YAP1 (54 kDa, Rabbit polyclonal antibody) (1:2000; Affinity Biosciences Cat# AF3328, RRID: AB_2810276), YAP1 (54 kDa, Rabbit polyclonal antibody) (1:2000; Affinity Biosciences Cat# AF6328, RRID: AB_ 2835184), activating transcription factor 4 (ATF4) (39 kDa, Rabbit polyclonal antibody) (1:2000; Affinity Biosciences Cat# DF6008, RRID: AB_2833025), solute carrier family 1 member 5 (SLC1A5) (56 kDa, Rabbit polyclonal antibody) (1:1000; Affinity Biosciences Cat# AF6610, RRID: AB_2843431), gamma histone (γH2Ax) (15 kDa, Rabbit monoclonal antibody) (1:5000; Abcam Cat# ab81299, RRID: AB_1640564), ERCC excision repair 1 (ERCC1) (36 kDa, Rabbit polyclonal antibody) (1:2000; Affinity Biosciences Cat# AF0154, RRID: AB_2833335), and glyceraldehyde-3-phosphate dehydrogenase (GAPDH) (37 kDa, Rabbit polyclonal antibody) (1:10 000; Affinity Biosciences Cat# AF7021, RRID: AB_2839421) by a gel image processing system (610020-9Q, Clinx, China). GAPDH is the loading control.

Statistical analysis

IBM SPSS Statistics (version 25.0, RRID: SCR_019096; IBM, USA) was used for statistical analyses. GraphPad Prism (version

9.0, RRID: SCR_002798; GraphPad Software, USA) was used to plot bar graphs and inhibition rate curves and to calculate the IC_{50}. Data for multiple groups were analysed using one-way analysis of variance (ANOVA) with the post hoc Tukey test. Data are shown as mean ± standard deviation. $P < 0.05$ indicates statistically significant.

Results

The antagonism of BBD to cisplatin resistance and GSH synthesis of CCAs

The CCK-8 assay was used to compare the IC_{50} values and inhibition rates between CCAs treated only with cisplatin and those subjected to co-treatment with BBD/cisplatin. The IC_{50} of cisplatin in CCAs is 118.8 μg/mL (Figure 1(a)). In particular, when CCAs were exposed to 0.25, 0.5, and 1 mg/mL of BBD together with cisplatin treatment, a significant increase was observed in the inhibition ratio of cisplatin (IC_{50}) on CCAs ($p < 0.01$) (Figure 1(b)). The co-treatment of cisplatin-resistant CCAs with BBD and cisplatin reduced the IC_{50} of cisplatin to 61.83 μg/mL (Figure 1(c)), indicating a reversal fold of 1.92. The enhanced apoptosis of CCAs was induced by cisplatin treatment ($p < 0.01$). The presence of 0.25, 0.5, and 1 mg/mL of BBD significantly increased apoptosis in CCAs subjected to cisplatin treatment ($p < 0.05$ or $p < 0.01$) (Figure 1(d)). The impact of BBD on GSH synthesis in CCAs was explored by measuring TTGSH, GSH, GSH/GSSG, and GLS levels (Figures 1(e–h)). Cisplatin treatment significantly decreased the relative activity of TTGSH, GSH/GSSG, and GLS in CCAs ($p < 0.01$) (Figures 1(e, f), and h)). In a dose-dependent manner, BBD reduced TTGSH, GSH/GSSG, and the relative activity of GLS in cisplatin-incubated CAAs ($p < 0.01$) (Figures 1(e, f, and h)). These findings showed that BBD enhanced the sensitivity of CCAs to cisplatin, promoted apoptosis in CCAs, and inhibited GSH levels.

Cisplatin and BBD co-treatment promoted DNA damage in CCAs

The comet assay was used to explore DNA damage in CCAs. Cell DNA damage is an important indicator in estimating cell sensitivity to chemotherapy (Goldstein and Kastan 2015). Cisplatin increased tail moment and tail DNA proportion in CCAs. Co-cultured BBD with cisplatin increased the tail moment and tail DNA compared to cisplatin treatment alone ($p < 0.05$ or $p < 0.01$) (Figures 2(a–c)). BBD exacerbated DNA damage to CCAs.

BBD regulated the signal strength of apoptosis, GSH synthesis, and the expression of DNA damage-related protein

We measured proteins associated with apoptosis (Figures 3(a–c and i)). In CCAs, cisplatin increased the signal strength of Bax expression ($p < 0.05$) (Figure 3(b)). An increase in cle-caspase-3/caspase-3 levels was observed in CCAs subjected to cisplatin treatment (Figure 1(c)), while the signal strength of Bcl-2 was significantly suppressed ($p < 0.01$) (Figure 1(a)). In particular, treatment with 0.25, 0.5, and 1 mg/mL BBD increased Bax levels within CCAs exposed to cisplatin ($p < 0.01$) (Figure 3(b)). In contrast, the alteration in Bcl-2 expression exhibited a trend opposite to that of Bax, except for the 0.25 mg/mL BBD treatment, which did not show significant differences ($p < 0.05$ or $p < 0.01$) (Figure 3(e)).

Furthermore, the expression levels of YAP1, ATF4, and SLC1A5 were examined to elucidate the role of BBD in GSH synthesis within CCAs (Figures 3(d–f and j)). The p-YAP1/YAP1 ratio in CCAs was significantly reduced due to cisplatin treatment ($p < 0.05$), and the same ratio within CCAs co-treated with cisplatin. BBD decreased markedly compared to cisplatin treatment alone ($p < 0.01$) (Figure 3(d)). Although cisplatin treatment alone increased the intensity of SLC1A5 and ATF4 signal in CCAs, co-treatment with cisplatin and BBD (at 0.25, 0.5, and 1 mg/mL) effectively reversed this effect ($p < 0.05$ or $p < 0.01$) (Figures 3(e and f)). Furthermore, the presence of γH2Ax exhibited a substantial increase in CCAs subjected to cisplatin and BBD co-treatment. In contrast, ERCC1 was suppressed in CCAs due to cisplatin treatment and showed a reduction when CCAs were subjected to cisplatin and BBD co-treatment compared to the cisplatin-only group ($p < 0.05$ or $p < 0.01$) (Figures 3(g, h and 3k)). Thus, BBD can potentially modulate the expression levels of proteins related to apoptosis, DNA damage, and GSH synthesis. This modulation appears to enhance the sensitivity of CCAs to cisplatin treatment.

YAP1 overexpression partially antagonized the facilitatory effect of BBD on the cisplatin sensitivity in CCAs

We explored the role of YAP1 in the antagonism of BBD on cisplatin resistance by constructing a YAP1 knockdown or overexpression CCA model through transfection. The qPCR results demonstrated that siYAP1-1/2/3 significantly suppressed transcription levels of YAP1. In contrast, YAP1-cDNA 1/2/3 led to an increase in these levels, with statistical significance ($p < 0.01$) as shown in Figures 4(a and b). In particular, siYAP1-1 and YAP1-cDNA 2 were more effective in modulating YAP1 expression. Consequently, these specific constructs were selected for use in subsequent experiments, with their effects also being statistically significant ($p < 0.01$) as shown in Figures 4(a and b). The inhibition ratio was significantly higher in YAP1 knockdown CCAs than in those treated with cisplatin ($p < 0.01$). Similarly, the inhibition ratio in CCAs with cisplatin and BBD co-treatment was higher than that of cisplatin-treated CCAs ($p < 0.01$) (Figure 4(c)). However, YAP1 overexpression in CCAs reversed the inhibition ratio in CCAs with cisplatin and BBD co-treatment ($p < 0.01$) (Figure 4(c)). In addition, flow cytometry was used to detect the level of apoptosis. YAP1 knockdown significantly increased apoptosis in cisplatin-incubated CCAs ($p < 0.01$), and BBD treatment increased the apoptosis in cisplatin-incubated CCAs ($p < 0.01$). In contrast, YAP1 overexpression markedly decreased apoptosis in CCAs with cisplatin and BBD co-treatment ($p < 0.01$) (Figures 4(d and e)). YAP1 overexpression partially antagonized the effects of BBD on inhibition ratio and apoptosis.

YAP1 overexpression antagonized the inhibitory effect of BBD on GSH synthesis in cisplatin-resistant CCAs

GSH/GSSG is an indicator of cell health (Owen and Butterfield 2010), and a high level of GSH plays an important role in multidrug resistance of cancer cells (Xiao et al. 2021). TTGSH, GLS, GSH, and GSH/GSSG levels in cisplatin-exposed CCAs were suppressed after YAP1 knockdown or treatment with 1 mg/mL BBD ($p < 0.05$ or $p < 0.01$). In contrast, these levels were elevated in CCAs overexpressing YAP1 and co-treated with cisplatin and BBD ($p < 0.01$, Figures 4(f–i)). YAP1 overexpression reversed the effects of BBD on GSH synthesis.

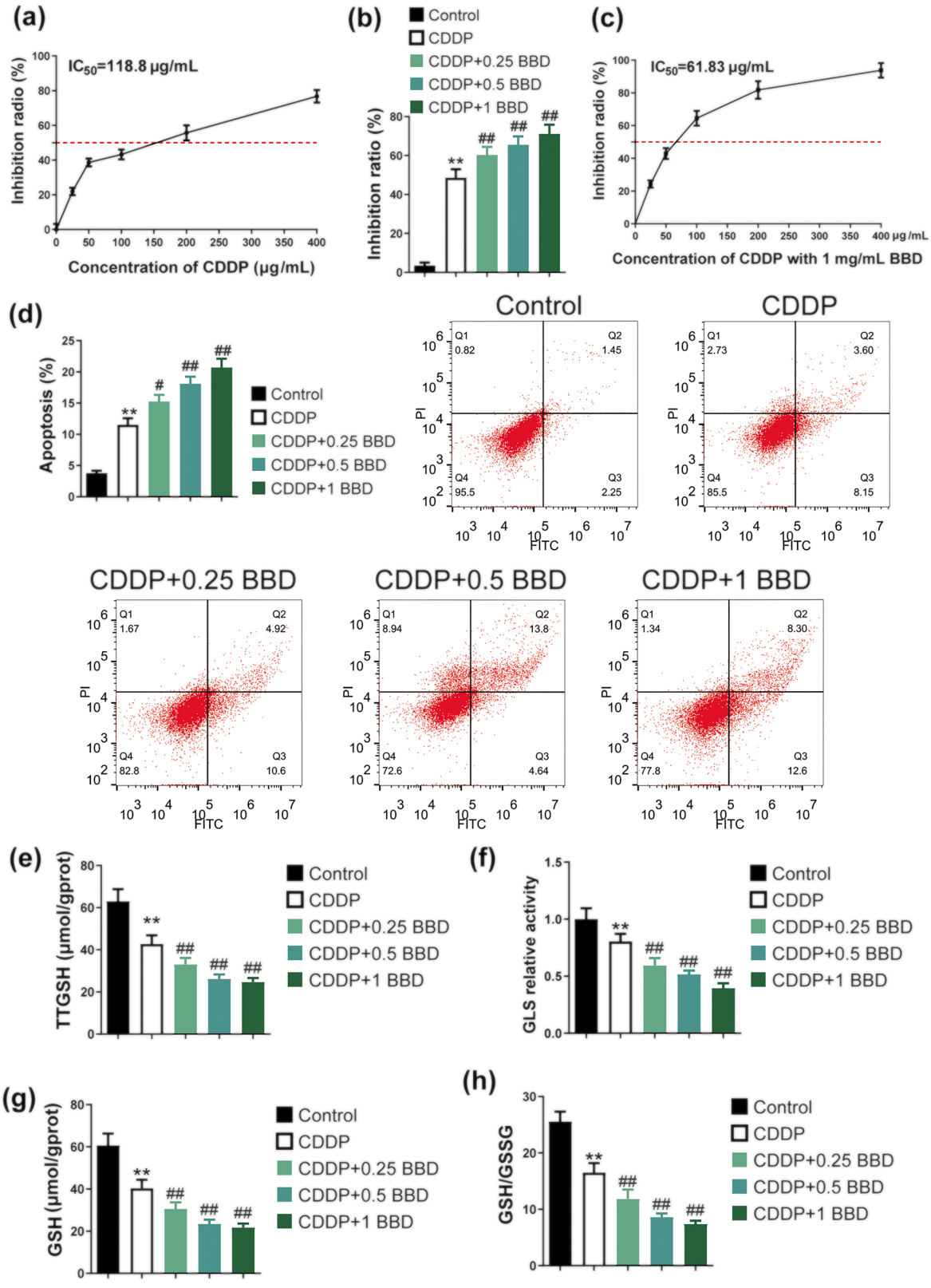

Figure 1. Babaodan (BBD) antagonized cisplatin resistance in cholangiocarcinoma cells (CCAs) by advancing the inhibition ratio, apoptosis, and inhibiting glutathione (GSH) synthesis. (a) The inhibition ratio curve and the IC_{50} of cisplatin in CCAs were measured using the cell counting kit 8 ($n = 5$). (b) according to the inhibition of cisplatin and cisplatin with BBD, 1 mg/mL of BBD was chosen for the follow-up study ($n = 5$). (c) the inhibition ratio curve and the IC_{50} of cisplatin with 1 mg/mL BBD in CCAs were also measured using the cell counting kit 8 ($n = 5$), and the IC_{50} was significantly reduced compared to cisplatin treatment alone. (d) The apoptosis of CCAs was detected by flow cytometry ($n = 3$). BBD increased apoptosis levels in a dose-dependent manner. (e) TTGSH, (f) relative activity of GLS, (g) GSH, and (h) GSH/GSSG levels in CCAs with cisplatin treatment were inhibited by BBD treatment in a dose-dependent manner. (mean ± standard deviation) $^{*}p < 0.05$, $^{**}p < 0.01$, *vs.* control group; $^{\#}p < 0.05$, $^{\#\#}p < 0.01$, *vs.* CDDP group.

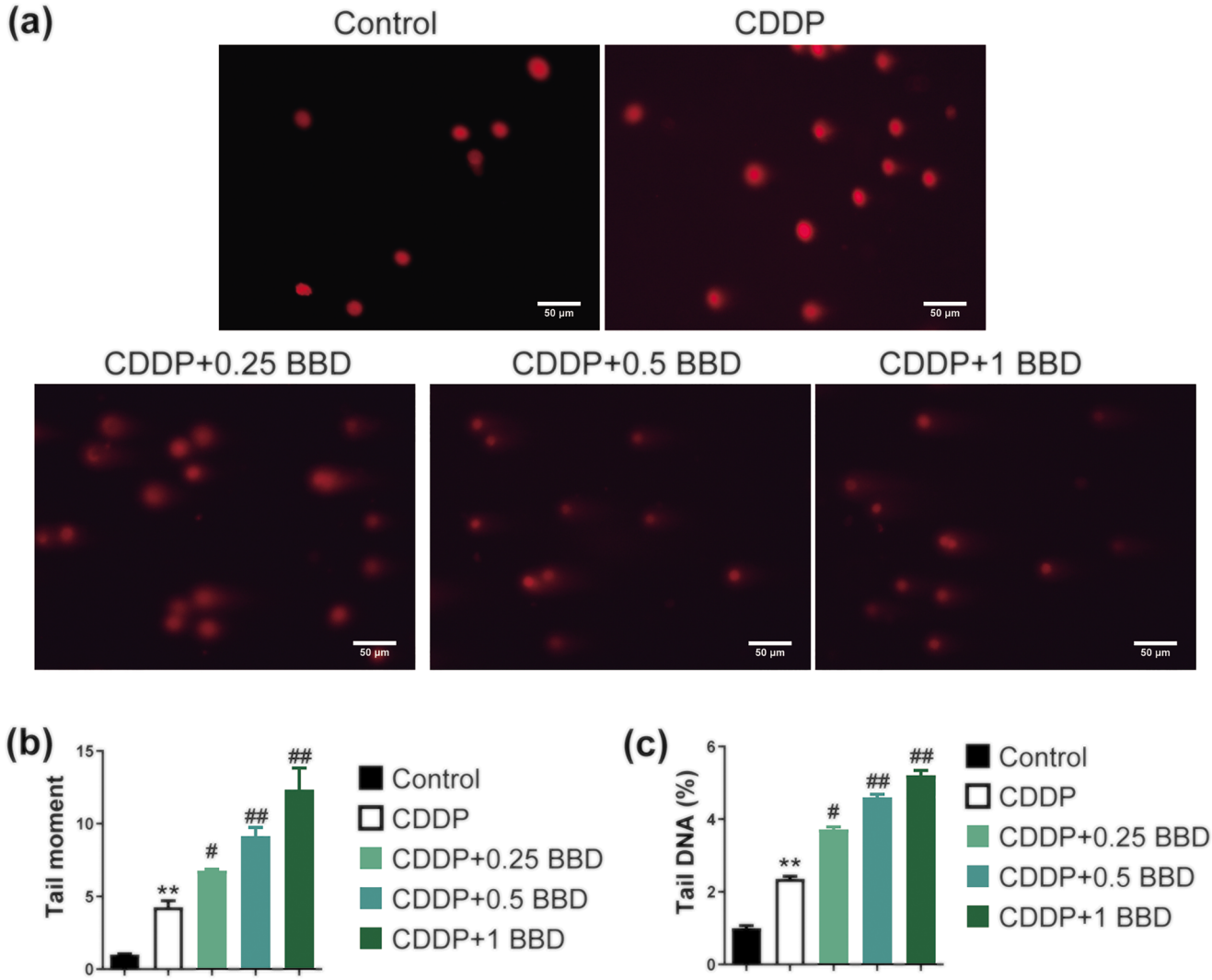

Figure 2. Babaodan (BBD) promoted the effect of cisplatin on DNA damage in cholangiocarcinoma cells (CCAs). (a) characteristic photos showed the DNA damage (×400, scale bar = 50 μm). The comet assay measured (b) the tail moment and (c) the percentage of tail DNA. The combination of cisplatin and BBD increased them compared to cisplatin alone ($n = 3$). (mean ± standard deviation) $^{*}p < 0.05$, $^{**}p < 0.01$, *vs.* control group; $^{\#}p < 0.05$, $^{\#\#}p < 0.01$, *vs.* CDDP group.

BBD inhibited YAP1 to enhance DNA damage in cisplatin-resistant CCAs

The comet assay was used to observe DNA damage in CCAs (Figures 5(a–c)). In YAP1-silenced CCAs with cisplatin incubation, the tail moment and tail DNA were significantly higher than CCAs ($p < 0.01$) (Figures 5(b and c)). Additionally, 1 mg/mL BBD treatment in CCAs under cisplatin incubation also increased the tail moment and tail DNA. In contrast, YAP1 overexpression antagonized the effect of BBD ($p < 0.01$) (Figures 5(b and c)). YAP1 overexpression antagonized BBD enhancement in DNA damage.

YAP1 overexpression regulated apoptosis, GSH synthesis, and DNA damage-related protein expression in cisplatin-resistant CCAs with cisplatin and BBD co-treatment

Upon cisplatin incubation, the Bcl-2 levels in YAP1-silenced CCAs were significantly decreased compared to control CCAs ($p < 0.01$) (Figures 6(a and i)). Additionally, YAP1 knockdown increased the levels of Bax and cle-caspase-3 in CCAs ($p < 0.05$ or $p < 0.01$) (Figures 6(b, c, and i)). Moreover, previous studies have associated YAP1, ATF4, and SLC1A5 with GSH synthesis (Hu et al. 2019). The expression signal intensities of p-YAP1/YAP1, ATF4, and SLC1A5 in CCAs subjected to cisplatin incubation were suppressed by silencing YAP1 or treatment with 1 mg/mL BBD ($p < 0.05$ or $p < 0.01$). In particular, YAP1 overexpression counteracted the inhibitory effects of 1 mg/mL BBD on these protein expressions in CCAs (Figures 6(d–f) and j). Furthermore, in CCAs incubated with cisplatin, the marker protein for DNA damage, γH2Ax, exhibited increased levels after YAP1 knockdown or 1 mg/mL of BBD treatment ($p < 0.05$ or $p < 0.01$). In contrast, the DNA excision repair protein ERCC1 was inhibited ($p < 0.01$) (Figures 6(g, h, and k)). YAP1 overexpression reversed the effects of BBD on the marker protein for DNA damage ($p < 0.05$ or $p < 0.01$) (Figures 6(g and h)). BBD treatment effectively enhanced the regulation of cisplatin on apoptosis, DNA damage, and GSH synthesis-related protein expressions *via* YAP1, thus enhancing the susceptibility of CCAs to cisplatin.

Discussion

This study demonstrated the antagonistic effects of BBD on cisplatin-resistant CCAs. BBD was found to inhibit GSH synthesis, thus enhancing apoptosis and inducing DNA damage in CCAs when combined with cisplatin treatment. BBD exhibited a dose-dependent regulation of the Bcl-2/Bax pathway, a crucial

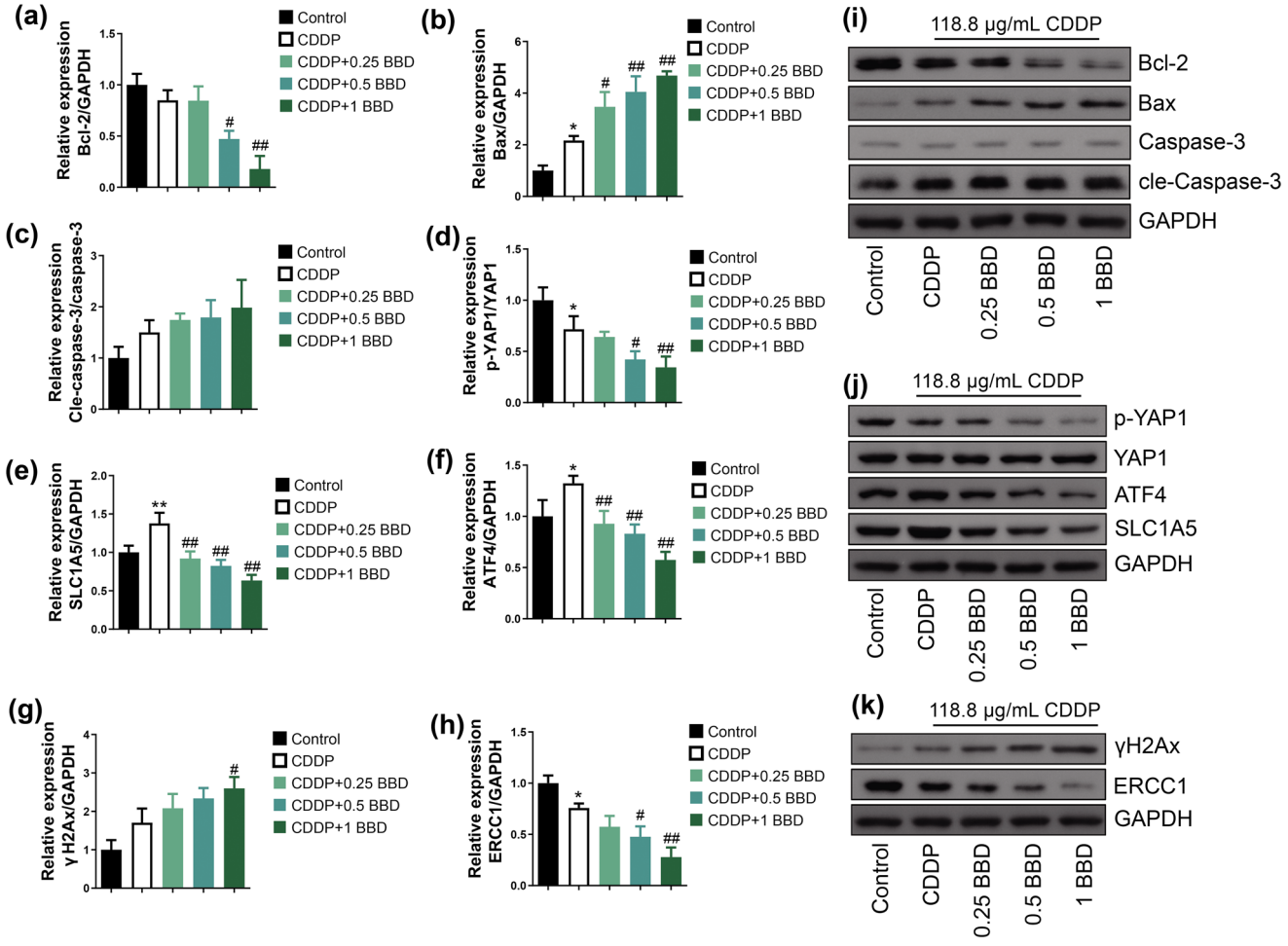

Figure 3. Apoptosis, glutathione (GSH) synthesis, and DNA damage-related protein expression in cholangiocarcinoma cells (CCAs) with co-treatment of babaodan (BBD) and cisplatin. Western blot was used to measure protein levels ($n = 3$). BBD decreased (a) the bcl-2 level and (b) increased the bax level in a dose-dependent manner. Change in (c) cle-caspase-3/caspase-3 levels with BBD treatment was not statistically significant. In CCAs involving cisplatin, the expression levels of (d) p-YAP1 relative to total YAP1, (e) SLC1A5, and (f) ATF4, which are involved in GSH synthesis, were observed to decrease in a dose-dependent manner following BBD treatment. (g) the γH2Ax level was increased by 1 mg/mL of BBD treatment, and (h) the ERCC1 level was inhibited by treatment with 0.5 and 1 mg/mL of BBD treatment. Representative protein bands are shown in the (i), (j), and (k). (mean ± Standard deviation) $^{*}p < 0.05$, $^{**}p < 0.01$, *vs.* control group; $^{\#}p < 0.05$, $^{\#\#}p < 0.01$, *vs.* CDDP group.

mediator of the intrinsic apoptotic cascade located in the outer mitochondrial membrane (Wilkins et al. 2012). Furthermore, increased Bax causes early cell apoptosis (Alam et al. 2022). A study (Yoon et al. 2011) reported that chemically resistant cells showed increased Bcl-2 and decreased Bax expression. Treatment with BBD inhibited Bcl-2 expression and increased Bax levels. The antagonistic effect of BBD on CCA cisplatin resistance may be related to the Bcl-2/Bax pathway.

YAP1 is a key effector molecule downstream of the Hippo signaling pathway that maintains organ size and tissue homeostasis through the orchestration of cell proliferation and apoptosis (He et al. 2020). A study (Sugiura et al. 2019) reported that patients with positive YAP expression had a poor prognosis in the Kaplan-Meier analysis. Targeting YAP1 promoted neuroblastoma cell apoptosis (Yang et al. 2021). Furthermore, inhibition of the YAP1 pathway promoted apoptosis in gastric cancer cells (Yao et al. 2021). The qPCR experiment results showed that we successfully established cell models with YAP1 knockdown or overexpression. Our study showed how YAP1 knockdown upregulated apoptosis while YAP1 overexpression partially counteracted the pro-apoptotic effects of BBD. Currently, the evidence supporting the role of YAP1 in promoting CCA proliferation is inadequate. Our study contributes a portion of the research foundation to address this gap. Our study demonstrated that BBD's antagonistic effects on cisplatin resistance in CCAs may be attributed to its inhibition of YAP1.

The antioxidant GSH maintains cellular redox homeostasis in living organisms (Bansal and Simon 2018). GSSG is the oxidized species of GSH. The elevated GSH/GSSG ratio within the nucleus plays a critical role in facilitating accurate nucleic acid biosynthesis and effective DNA repair processes (Bansal and Simon 2018). Activated GLS promotes tumor cell survival and tumor growth in mice by increasing GSH (Tong et al. 2021). In addition, tumor progression and increased resistance to chemotherapeutic drugs are associated with elevated GSH levels in cells (Kennedy et al. 2020). Interruption of the GSH and mitochondrial pathway induced apoptosis and inhibited CCA resistance (Tusskorn et al. 2013). YAP1 expression can activate the ATF/SLC7A11 pathway to promote GSH synthesis (Gao et al. 2021; Mohajan et al. 2021). Silenced YAP1 can affect the expression of SLC1A5, significantly reduce intracellular glutamine (one of the precursors of GSH synthesis) transfer and affect GSH synthesis (Edwards et al. 2017). Moreover, SLC1A5 overexpression leads to tolerance to pancreatic cancer chemotherapy (Yoo et al. 2020; Teixeira et al.

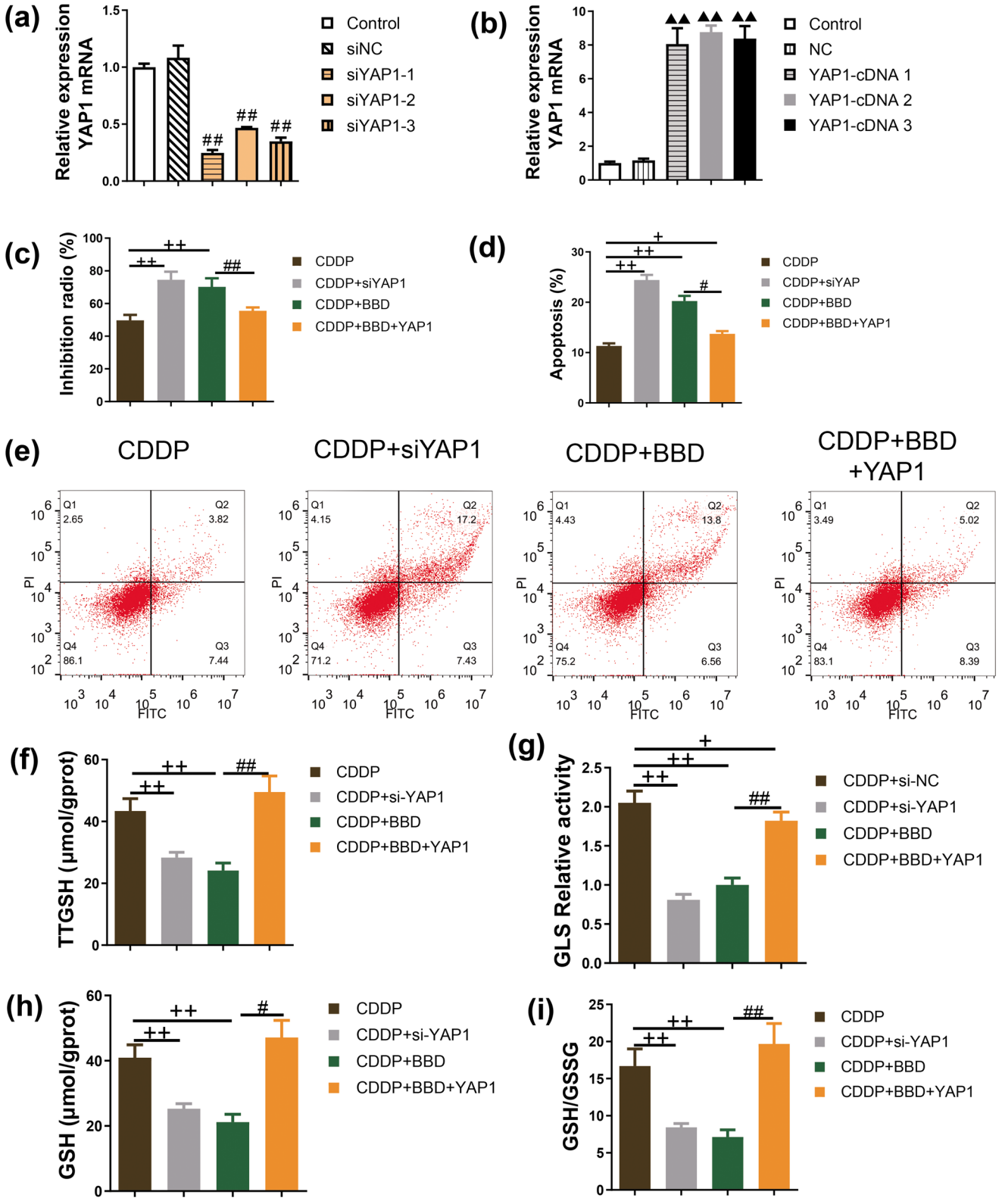

Figure 4. Babaodan (BBD) antagonized cisplatin resistance in cholangiocarcinoma cells (CCAs) by inhibiting YAP1. (a, b) The YAP1 mRNA of CCAs with siYAP1 and YAP1 cDNA transfection was measured using quantitative real-time PCR ($n = 3$). $^{\#\#}p < 0.01$ *vs.* siNC group; $^{\blacktriangle\blacktriangle}p < 0.01$ *vs.* NC group. (c) The inhibition ratio was detected using the cell counting kit 8 ($n = 5$). (d) apoptosis was measured by flow cytometry ($n = 3$) and increased in CCAs with YAP1 knockdown. Additionally, YAP1 overexpression antagonized the inhibition effect of BBD on CCA proliferation with cisplatin treatment. (e) Representative images of flow cytometry are shown. The levels of (f) TTGSH, (g) relative activity of GLS, (h) GSH, and (i) GSH/GSSG in CCAs with YAP1 knockdown, and cisplatin/BBD co-treatment were decreased and were reversed by YAP1 overexpression ($n = 5$). (mean ± standard deviation) $^{+}p < 0.05$, $^{++}p < 0.01$ *vs.* CDDP group; $^{\#}p < 0.05$, $^{\#\#}p < 0.01$, *vs.* CDDP + BBD group.

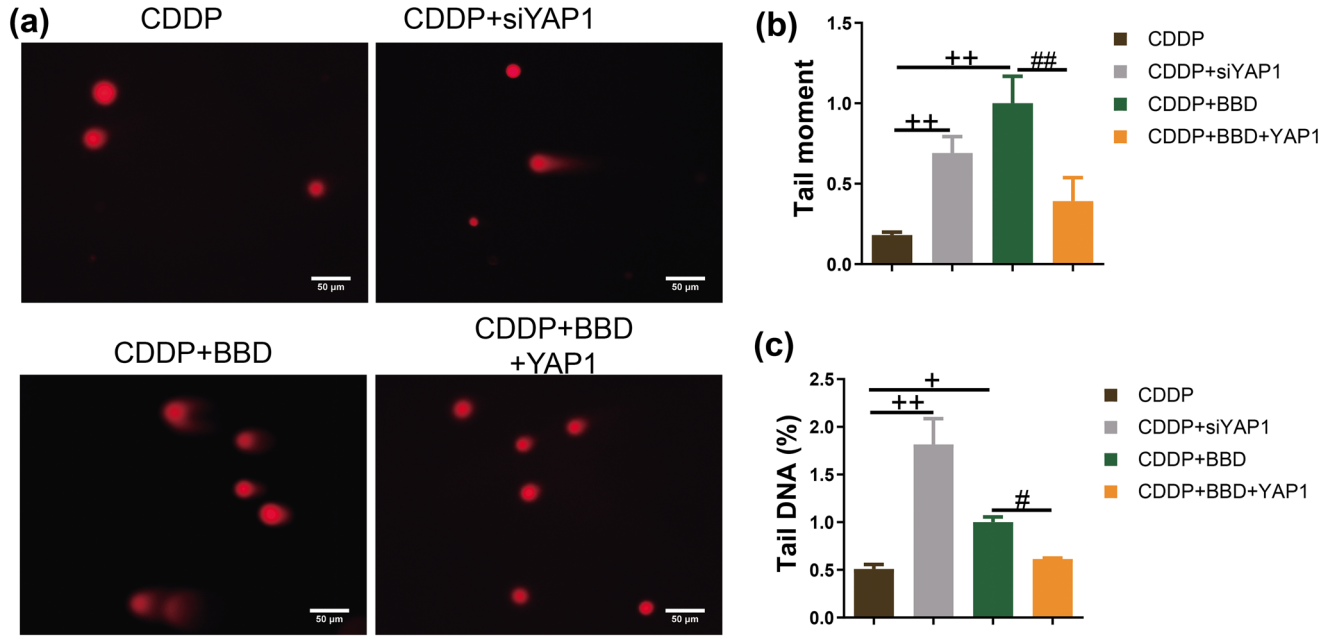

Figure 5. YAP1 Overexpression antagonized the promotional effect of babaodan (BBD) on DNA damage in cholangiocarcinoma cells with cisplatin. (a) The characteristic photos showed the DNA damage (×400, scale bar = 50 μm). The comet assay was used to measure (b) tail moment and (c) percentage of tail DNA, and YAP1 overexpression inhibited (b) tail moment and (c) percentage of tail DNA in cholangiocarcinoma cells with co-treatment of cisplatin and BBD ($n = 3$). (mean ± standard deviation) $^{+}p < 0.05$, $^{++}p < 0.01$, *vs.* CDDP group; $^{\#}p < 0.05$, $^{\#\#}p < 0.01$, *vs.* CDDP + BBD group.

2021). Abnormal activation of YAP1 is associated with intrahepatic cholangiocarcinoma (Zhang Y et al. 2022). The proto-oncogene Bcl-2 inhibits apoptosis activation, contributes to GSH elevation, and is directly associated with resistance (Xu and Ye 2022). We found that BBD decreased the GSH level, which may be related to the inhibition of BBD on the expression strength of the YAP1/ATF4/SLC1A5 signal. In addition, BBD promoted the oxidation of GSH to GSSG. YAP1 has been found to regulate the GSSG level in the yeast *Pichia pastoris* (Delic et al. 2014). The role of YAP1 in the GSH synthesis of CCA deserves further exploration.

Studies (Huang et al. 2018; Chaouhan et al. 2021) have reported that loss of GSH promotes the occurrence of DNA damage, and increasing GSH synthesis can alleviate DNA damage. Cellular responses to DNA damage are important determinants of cancer development and outcome after radiation therapy and chemotherapy (Goldstein and Kastan 2015). Therefore, this study observed the tail moment and the proportion of tail DNA to evaluate DNA damage in CCAs. The γH2Ax is a biomarker of DNA double-strand breaks (Rothkamm et al. 2015). In addition, Ercc1 is a DNA excision repair protein necessary for DNA damage repair (Zhang et al. 2021). The strength of the γH2Ax signal expression exhibited a dose-dependent increase, accompanied by a reduction in Ercc1 expression after BBD treatment.

YAP1 overexpression counteracted these effects, implying that BBD can enhance CCA susceptibility to cisplatin, with YAP1 playing a participatory role in this process. YAP1 knockdown and BBD treatment constrained GSH synthesis in cisplatin-resistant CCAs. In particular, YAP1 overexpression counteracted the impact of BBD on GSH synthesis. These findings imply that YAP1 can potentially promote apoptosis, DNA damage, and GSH depletion as a strategic approach to overcome cisplatin resistance in CCAs, achieved by inhibiting YAP1. This study clarified the potential of BBD to improve the sensitivity of CCAs to cisplatin.

This study has limitations. BBD is a TCM compound recipe with complex active ingredients. A UPLC-QTOF-MS analysis of BBD reported 85 chemicals, including 24 cholic acids, 33 saponins, and 15 fatty acids (Sheng et al. 2022). Taurocholic acid and glycocholic acid were identified as the primary bile acids in BBD with anti-inflammatory effects (Ge et al. 2023). The active ingredient of BBD, ginsenoside compound K, inhibited the growth of hepatocellular carcinoma by regulating the phosphorylation of YAP1 (Zhang J et al. 2022). However, research on the main active ingredients of BBD with anti-tumor activities is still lacking. It is necessary to further explore the blood components of BBD and related mechanisms to provide basic data for further clinical drug application and development.

Conclusions

This study proved that BBD increased the sensitivity of CCAs to cisplatin. BBD treatment decreased cisplatin IC_{50}, increased apoptosis rate, and DNA damage in CCAs with cisplatin treatment. Administration of BBD to cisplatin-resistant CCAs, in conjunction with cisplatin incubation, reduced expression levels for Bcl-2, p-YAP1/YAP1, SLC1A5, ATF4, and ERCC1. Simultaneously, it increased the expression of Bax and γH2Ax. In particular, YAP1 knockdown in cisplatin-resistant CCAs had a similar effect to BBD. They inhibited GSH, GSH-oxidized species, total GSH, and glutaminase. At the same time, YAP1 overexpression antagonized the impact of BBD on cisplatin-resistant CCAs, suggesting that BBD may inhibit YAP1 to improve the sensitivity of CCAs to cisplatin. This study provides a scientific basis for expanding the clinical application of BBD. Additionally, it is essential to note that this study constitutes fundamental research focused on CCAs. Further support through clinical trials is warranted to expand its applicability to a broader population.

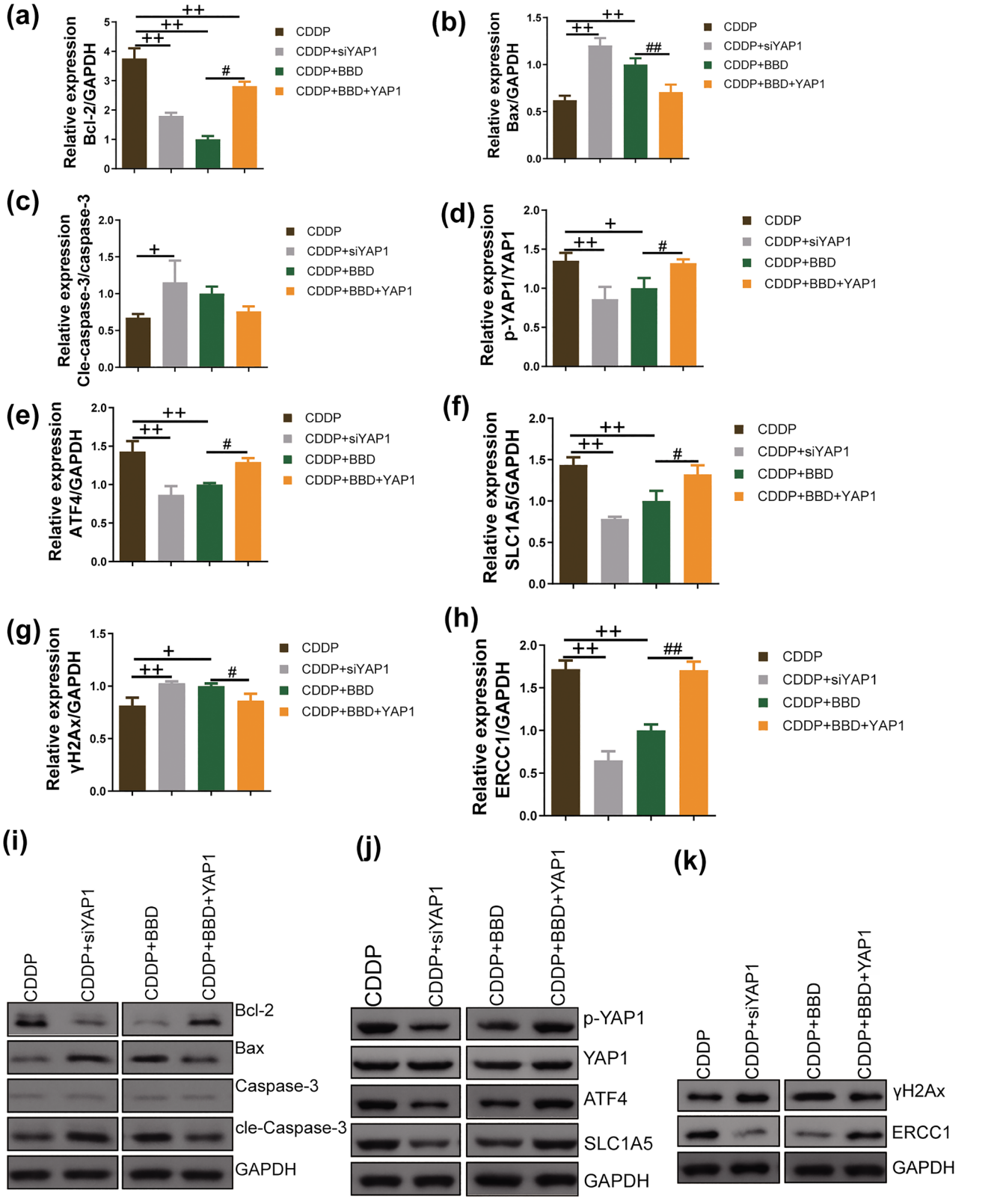

Figure 6. The extent of apoptosis, glutathione (GSH) synthesis, and the expression of DNA damage-related proteins were assessed in cholangiocarcinoma cells (CCAs) subjected to YAP1 knockdown or YAP1 overexpression. Western blot was used to measure protein levels ($n = 3$). With cisplatin incubation, YAP1 knockdown and 1 mg/mL babaodan (BBD) treatment decreased the (a) Bcl-2 level and (b) increased bax level, while the change in (c) cle-caspase-3/caspase-3 levels with BBD treatment was not statistically significant. In the CCAs dealing with cisplatin, the expression levels of (d) p-YAP1/YAP1, (e) ATF4, and (f) SLC1A5 were decreased by YAP1 knockdown and BBD treatment. Additionally, the (g) γH2Ax level was increased and (h) the ERCC1 level was inhibited by YAP1 knockdown and BBD treatment. YAP1 overexpression antagonized the effect of BBD on these proteins. Representative protein bands are shown in (i), (j), and (k). (mean ± standard deviation) $^{+}p < 0.05$, $^{++}p < 0.01$, *vs.* CDDP group; $^{\#}p < 0.05$, $^{\#\#}p < 0.01$, *vs.* CDDP + BBD group.

Disclosure statement

The authors report there are no competing interests to declare.

Author contribution statement

Jiong Li: Data curation, Methodology, Validation, Writing-original draft, Writing-review & editing; Xiangjun Ma: Data curation, Formal analysis, Methodology, Writing-original draft; Faying Xu: Formal analysis, Methodology, Writing-original draft; Yuanliang Yan: Writing-original draft, Funding acquisition, Project administration, Resources, Supervision; Weiqing Chen: Writing-original draft, Funding acquisition, Project administration, Supervision, Writing-review & editing.

Funding

This work was supported by the Hangzhou Agricultural and Social Development Research Guidance Project [grant number 20220919Y128].

Data availability statement

The authors confirm that the data supporting the findings of this study are available within its supplementary materials.

References

Alam M, Alam S, Shamsi A, Adnan M, Elasbali AM, Al-Soud WA, Alreshidi M, Hawsawi YM, Tippana A, Pasupuleti VR, et al. 2022. Bax/Bcl-2 Cascade is regulated by the EGFR pathway: therapeutic targeting of non-small cell lung cancer. Front Oncol. 12:869672. doi: 10.3389/fonc.2022.869672.

Banales JM, Marin JJG, Lamarca A, Rodrigues PM, Khan SA, Roberts LR, Cardinale V, Carpino G, Andersen JB, Braconi C, et al. 2020. Cholangiocarcinoma 2020: the next horizon in mechanisms and management. Nat Rev Gastroenterol Hepatol. 17(9):557–588. doi: 10.1038/s41575-020-0310-z.

Bansal A, Simon MC. 2018. Glutathione metabolism in cancer progression and treatment resistance. J Cell Biol. 217(7):2291–2298. doi: 10.1083/jcb.201804161.

Chaouhan HS, Jha RR, Patel DK, Kar Chowdhuri D. 2021. Cr^{VI}-induced DNA damage is lessened by the modulation of hsp70 via increased GSH *de novo* synthesis in *Drosophila melanogaster*. J Biochem Mol Toxicol. 35(8):e22819. doi: 10.1002/jbt.22819.

Chen P, Liu XQ, Lin X, Gao LY, Zhang S, Huang X. 2021. Targeting YTHDF1 effectively re-sensitizes cisplatin-resistant colon cancer cells by modulating GLS-mediated glutamine metabolism. Mol Ther Oncolytics. 20:228–239. doi: 10.1016/j.omto.2021.01.001.

Chen Z, Lin T, Liao X, Li Z, Lin R, Qi X, Chen G, Sun L, Lin L. 2021. Network pharmacology based research into the effect and mechanism of Yinchenhao Decoction against cholangiocarcinoma. Chin Med. 16(1):13. doi: 10.1186/s13020-021-00423-4.

Ciamporcero E, Daga M, Pizzimenti S, Roetto A, Dianzani C, Compagnone A, Palmieri A, Ullio C, Cangemi L, Pili R, et al. 2018. Crosstalk between Nrf2 and YAP contributes to maintaining the antioxidant potential and chemoresistance in bladder cancer. Free Radic Biol Med. 115:447–457. doi: 10.1016/j.freeradbiomed.2017.12.005.

Delic M, Graf AB, Koellensperger G, Haberhauer-Troyer C, Hann S, Mattanovich D, Gasser B. 2014. Overexpression of the transcription factor Yap1 modifies intracellular redox conditions and enhances recombinant protein secretion. Microb Cell. 1(11):376–386. doi: 10.15698/mic2014.11.173.

Dwyer BJ, Jarman EJ, Gogoi-Tiwari J, Ferreira-Gonzalez S, Boulter L, Guest RV, Kendall TJ, Kurian D, Kilpatrick AM, Robson AJ, et al. 2021. TWEAK/Fn14 signalling promotes cholangiocarcinoma niche formation and progression. J Hepatol. 74(4):860–872. doi: 10.1016/j.jhep.2020.11.018.

Edwards DN, Ngwa VM, Wang S, Shiuan E, Brantley-Sieders DM, Kim LC, Reynolds AB, Chen J. 2017. The receptor tyrosine kinase EphA2 promotes glutamine metabolism in tumors by activating the transcriptional coactivators YAP and TAZ. Sci Signal. 10(508):eaan4667. doi: 10.1126/scisignal.aan4667.

Gao R, Kalathur RKR, Coto-Llerena M, Ercan C, Buechel D, Shuang S, Piscuoglio S, Dill MT, Camargo FD, Christofori G, et al. 2021. YAP/TAZ and ATF4 drive resistance to Sorafenib in hepatocellular carcinoma by preventing ferroptosis. EMBO Mol Med. 13(12):e14351. doi: 10.15252/emmm.202114351.

Ge X, Huang S, Ren C, Zhao L. 2023. Taurocholic acid and glycocholic acid inhibit inflammation and activate farnesoid X receptor expression in LPS-stimulated zebrafish and macrophages. Molecules. 28(5):2005. doi: 10.3390/molecules28052005.

Ghosh S. 2019. Cisplatin: the first metal based anticancer drug. Bioorg Chem. 88:102925. doi: 10.1016/j.bioorg.2019.102925.

Goldstein M, Kastan MB. 2015. The DNA damage response: implications for tumor responses to radiation and chemotherapy. Annu Rev Med. 66(1):129–143. doi: 10.1146/annurev-med-081313-121208.

Guedj N. 2022. Pathology of cholangiocarcinomas. Curr Oncol. 30(1):370–380. doi: 10.3390/curroncol30010030.

He L, Yuan L, Yu W, Sun Y, Jiang D, Wang X, Feng X, Wang Z, Xu J, Yang R, et al. 2020. A regulation loop between YAP and NR4A1 balances cell proliferation and apoptosis. Cell Rep. 33(3):108284. doi: 10.1016/j.celrep.2020.108284.

Hu X, Deng J, Yu T, Chen S, Ge Y, Zhou Z, Guo Y, Ying H, Zhai Q, Chen Y, et al. 2019. ATF4 deficiency promotes intestinal inflammation in mice by reducing uptake of glutamine and expression of antimicrobial peptides. Gastroenterology. 156(4):1098–1111. doi: 10.1053/j.gastro.2018.11.033.

Huang D, Zhang X, Zhang C, Li H, Li D, Hu Y, Yang F, Qi Y. 2018. 2,4-Dichlorophenol induces DNA damage through ROS accumulation and GSH depletion in goldfish *Carassius auratus*. Environ Mol Mutagen. 59(9):798–804. doi: 10.1002/em.22209.

Jia Y, Zhang W, Liu H, Peng L, Yang Z, Lou J. 2012. Inhibition of glutathione synthesis reverses Krüppel-like factor 4-mediated cisplatin resistance. Cancer Chemother Pharmacol. 69(2):377–385. doi: 10.1007/s00280-011-1708-7.

Kennedy L, Sandhu JK, Harper ME, Cuperlovic-Culf M. 2020. Role of glutathione in cancer: from mechanisms to therapies. Biomolecules. 10(10):1429. doi: 10.3390/biom10101429.

Khan SA, Tavolari S, Brandi G. 2019. Cholangiocarcinoma: epidemiology and risk factors. Liver Int. 39 Suppl 1(S1):19–31. doi: 10.1111/liv.14095.

Kleih M, Böpple K, Dong M, Gaißler A, Heine S, Olayioye MA, Aulitzky WE, Essmann F. 2019. Direct impact of cisplatin on mitochondria induces ROS production that dictates cell fate of ovarian cancer cells. Cell Death Dis. 10(11):851. doi: 10.1038/s41419-019-2081-4.

Kobayashi M, Yonezawa A, Takasawa H, Nagao Y, Iguchi K, Endo S, Ikari A, Matsunaga T. 2022. Development of cisplatin resistance in breast cancer MCF7 cells by up-regulating aldo-keto reductase 1C3 expression, glutathione synthesis and proteasomal proteolysis. J Biochem. 171(1):97–108. doi: 10.1093/jb/mvab117.

Li Q, Zhan M, Chen W, Zhao B, Yang K, Yang J, Yi J, Huang Q, Mohan M, Hou Z, et al. 2016. Phenylethyl isothiocyanate reverses cisplatin resistance in biliary tract cancer cells via glutathionylation-dependent degradation of Mcl-1. Oncotarget. 7(9):10271–10282. doi: 10.18632/oncotarget.7171.

Liu CW, Hua KT, Li KC, Kao HF, Hong RL, Ko JY, Hsiao M, Kuo ML, Tan CT. 2017. Histone methyltransferase G9a drives chemotherapy resistance by regulating the glutamate-cysteine ligase catalytic subunit in head and neck squamous cell carcinoma. Mol Cancer Ther. 16(7):1421–1434. doi: 10.1158/1535-7163.MCT-16-0567-T.

Liu J, Chen Y, Cao Z, Guan B, Peng J, Chen Y, Zhan Z, Sferra TJ, Sankararaman S, Lin J. 2020. Babao Dan inhibits the migration and invasion of gastric cancer cells by suppressing epithelial-mesenchymal transition through the TGF-β/Smad pathway. J Int Med Res. 48(6):300060520925598. doi: 10.1177/0300060520925598.

Liu Z, Peng Q, Li Y, Gao Y. 2018. Resveratrol enhances cisplatin-induced apoptosis in human hepatoma cells via glutamine metabolism inhibition. BMB Rep. 51(9):474–479. doi: 10.5483/BMBRep.2018.51.9.114.

Mohajan S, Jaiswal PK, Vatanmakarian M, Yousefi H, Sankaralingam S, Alahari SK, Koul S, Koul HK. 2021. Hippo pathway: regulation, deregula-

tion and potential therapeutic targets in cancer. Cancer Lett. 507:112–123. doi: 10.1016/j.canlet.2021.03.006.

Owen JB, Butterfield DA. 2010. Measurement of oxidized/reduced glutathione ratio. Methods Mol Biol. 648:269–277. doi: 10.1007/978-1-60761-756-3_18.

Prasopporn S, Suppramote O, Ponvilawan B, Jamyuang C, Chanthercrob J, Chaiboonchoe A, More-Krong P, Kongsri K, Suntiparpluacha M, Chanwat R, et al. 2022. Combining the SMAC mimetic LCL161 with gemcitabine plus cisplatin therapy inhibits and prevents the emergence of multidrug resistance in cholangiocarcinoma. Front Oncol. 12:1021632. doi: 10.3389/fonc.2022.1021632.

Rizvi S, Khan SA, Hallemeier CL, Kelley RK, Gores GJ. 2018. Cholangiocarcinoma - evolving concepts and therapeutic strategies. Nat Rev Clin Oncol. 15(2):95–111. doi: 10.1038/nrclinonc.2017.157.

Rodrigues PM, Olaizola P, Paiva NA, Olaizola I, Agirre-Lizaso A, Landa A, Bujanda L, Perugorria MJ, Banales JM. 2021. Pathogenesis of cholangiocarcinoma. Annu Rev Pathol. 16(1):433–463. doi: 10.1146/annurev-pathol-030220-020455.

Rothkamm K, Barnard S, Moquet J, Ellender M, Rana Z, Burdak-Rothkamm S. 2015. DNA damage foci: meaning and significance. Environ Mol Mutagen. 56(6):491–504. doi: 10.1002/em.21944.

Sheng H, Li Y, Liu W, Wang Y, Wang S, Zhan Z, Lai Z, Guan B, Qiang S, Qian J, et al. 2022. Identification of bioactive ingredients from Babaodan using UPLC-QTOF-MS analysis combined with network pharmacology guided bioassays. J Chromatogr B Analyt Technol Biomed Life Sci. 1206:123356. doi: 10.1016/j.jchromb.2022.123356.

Sugiura K, Mishima T, Takano S, Yoshitomi H, Furukawa K, Takayashiki T, Kuboki S, Takada M, Miyazaki M, Ohtsuka M. 2019. The expression of Yes-associated protein (YAP) maintains putative cancer stemness and is associated with poor prognosis in intrahepatic cholangiocarcinoma. Am J Pathol. 189(9):1863–1877. doi: 10.1016/j.ajpath.2019.05.014.

Teixeira E, Silva C, Martel F. 2021. The role of the glutamine transporter ASCT2 in antineoplastic therapy. Cancer Chemother Pharmacol. 87(4):447–464. doi: 10.1007/s00280-020-04218-6.

Tong Y, Guo D, Lin SH, Liang J, Yang D, Ma C, Shao F, Li M, Yu Q, Jiang Y, et al. 2021. SUCLA2-coupled regulation of GLS succinylation and activity counteracts oxidative stress in tumor cells. Mol Cell. 81(11):2303–2316.e2308. doi: 10.1016/j.molcel.2021.04.002.

Tusskorn O, Prawan A, Senggunprai L, Kukongviriyapan U, Kukongviriyapan V. 2013. Phenethyl isothiocyanate induces apoptosis of cholangiocarcinoma cells through interruption of glutathione and mitochondrial pathway. Naunyn Schmiedebergs Arch Pharmacol. 386(11):1009–1016. doi: 10.1007/s00210-013-0906-8.

Wang Q, Liu Z, Du K, Liang M, Zhu X, Yu Z, Chen R, Qin L, Li Y, Zheng Y. 2019. Babaodan inhibits cell growth by inducing autophagy through the PI3K/AKT/mTOR pathway and enhances antitumor effects of cisplatin in NSCLC cells. Am J Transl Res. 11:5272–5283.

Wilkins HM, Marquardt K, Lash LH, Linseman DA. 2012. Bcl-2 is a novel interacting partner for the 2-oxoglutarate carrier and a key regulator of mitochondrial glutathione. Free Radic Biol Med. 52(2):410–419. doi: 10.1016/j.freeradbiomed.2011.10.495.

Xiao X, Wang K, Zong Q, Tu Y, Dong Y, Yuan Y. 2021. Polyprodrug with glutathione depletion and cascade drug activation for multi-drug resistance reversal. Biomaterials. 270:120649. doi: 10.1016/j.biomaterials.2020.120649.

Xu Y, Ye H. 2022. Progress in understanding the mechanisms of resistance to BCL-2 inhibitors. Exp Hematol Oncol. 11(1):31. doi: 10.1186/s40164-022-00283-0.

Yang L, He K, Yao S, Zhang Y, Shen J. 2021. Sevoflurane inhibits neuroblastoma cell proliferation and invasion and induces apoptosis by miR-144-3p/YAP1 axis. Basic Clin Pharmacol Toxicol. 129(4):297–307. doi: 10.1111/bcpt.13629.

Yao W, Guo P, Mu Q, Wang Y. 2021. Exosome-derived circ-PVT1 contributes to cisplatin resistance by regulating autophagy, invasion, and apoptosis via miR-30a-5p/YAP1 axis in gastric cancer cells. Cancer Biother Radiopharm. 36(4):347–359. doi: 10.1089/cbr.2020.3578.

Yoo HC, Park SJ, Nam M, Kang J, Kim K, Yeo JH, Kim JK, Heo Y, Lee HS, Lee MY, et al. 2020. A variant of SLC1A5 is a mitochondrial glutamine transporter for metabolic reprogramming in cancer cells. Cell Metab. 31(2):267–283.e212. doi: 10.1016/j.cmet.2019.11.020.

Yoon H, Min JK, Lee JW, Kim DG, Hong HJ. 2011. Acquisition of chemoresistance in intrahepatic cholangiocarcinoma cells by activation of AKT and extracellular signal-regulated kinase (ERK)1/2. Biochem Biophys Res Commun. 405(3):333–337. doi: 10.1016/j.bbrc.2010.11.130.

Zhang J, Tong Y, Lu X, Dong F, Ma X, Yin S, He Y, Liu Y, Liu Q, Fan D. 2022. A derivant of ginsenoside CK and its inhibitory effect on hepatocellular carcinoma. Life Sci. 304:120698. doi: 10.1016/j.lfs.2022.120698.

Zhang X, Heng Y, Kooistra SM, van Weering HRJ, Brummer ML, Gerrits E, Wesseling EM, Brouwer N, Nijboer TW, Dubbelaar ML, et al. 2021. Intrinsic DNA damage repair deficiency results in progressive microglia loss and replacement. Glia. 69(3):729–745. doi: 10.1002/glia.23925.

Zhang Y, Xu H, Cui G, Liang B, Chen X, Ko S, Affo S, Song X, Liao Y, Feng J, et al. 2022. β-Catenin sustains and is required for YES-associated protein oncogenic activity in cholangiocarcinoma. Gastroenterology. 163(2):481–494. doi: 10.1053/j.gastro.2022.04.028.

Zhao J, Lan W, Peng J, Guan B, Liu J, Zhang M, Zhan Z, Lin J. 2021. Babao Dan reverses multiple-drug resistance in gastric cancer cells via triggering apoptosis and autophagy and inhibiting PI3K/AKT/mTOR signaling. Evid Based Complement Alternat Med. 2021:5631942. doi: 10.1155/2021/5631942.

Zheng Q, Zhang B, Li C, Zhang X. 2022. Overcome drug resistance in cholangiocarcinoma: new insight into mechanisms and refining the preclinical experiment models. Front Oncol. 12:850732. doi: 10.3389/fonc.2022.850732.

Zheng Y, Lin Y, Zhu M, Chen T, Cheng Z, Lin Y, Huang JCM. 2022. Simultaneous determination of 15 bile acids in Babaodan by UPLC-MS/MS. J Pharm Anal. 42:2186–2194.

Zong C, Kimura Y, Kinoshita K, Takasu S, Zhang X, Sakurai T, Sekido Y, Ichihara S, Endo G, Ichihara G. 2019. Exposure to 1,2-dichloropropane upregulates the expression of activation-induced cytidine deaminase (AID) in human cholangiocytes co-cultured with macrophages. Toxicol Sci. 168(1):137–148. doi: 10.1093/toxsci/kfy280.